L'ÉLECTROMAGNÉTISME, 150-1
UNE SCIENCE EN PLEINE ACTION !

Near-field observation of beam steering in a photonic crystal superprism

Jean Dellinger[1], K. Van Do[2], Xavier Le Roux[2], Frédérique de Fornel[1], Eric Cassan[2],[*] Benoît Cluzel[1,]

1 Groupe d'Optique de Champ Proche –Laboratoire Interdisciplinaire Carnot de Bourgogne, UMR CNRS n°6303, université de Bourgogne, Dijon, France
2 Institut d'Electronique Fondamentale, Université Paris-Sud, CNRS, 91405 Orsay, France

Scanning Nearfield Optical Microscope, Hyperspectral imaging, Photonic crystals, Mirage effect
Microscopie en champ proche optique, Imagerie hyperspectrale, Cristaux photoniques, Effet mirage

Les matériaux artificiels réalisés pour les longueurs d'ondes optiques arrivent à un degré de maturité certain aussi bien dans leurs champs d'études que dans leurs applications.
A partir de cristaux photoniques à gradients il est ainsi possible de réaliser différentes fonctions optiques (séparateurs de polarisation, démultiplexeurs...). Nous présenterons donc l'étude théorique de telles structures, leur réalisation ainsi que leur caractérisation. La caractérisation se fera à l'aide d'un microscope en champ proche optique hyperspectral. L'usage de ce microscope particulier permet des études spectrales fines de composants fortement sensibles à la longueur d'onde. Nous montrerons l'accord entre simulations et mesures en champ proche, démontrant les propriétés particulières de ces structures à cristaux photoniques à gradient.

Artificial materials at optical frequencies have raised a strong interest in the last years, including photonic metamaterials, graded photonic crystals, and simple gradient index structures. The main common objective of these approaches is achieving a tight control of the electromagnetic guided-wave fields to play with light properties and propose versatile optical functions. In this general context, this work is focused on gradual photonic crystals (GPhCs) working in the diffraction regime, i.e. close to the photonic crystal (PhC) bandgap. A two-dimensional chirp of the PhC lattice parameters using a modelling approach based on Hamiltonian Optics (HO) was then proposed in [1] and far-field experimental observations of the light bending effect was shown in [2].

To provide in situ observations of the electromagnetic fields behavior inside these artificial structures and thus to improve our understanding of the involved light matter interactions, the scanning near-field optical microscopy (SNOM) techniques have raised an increasing interest over this last decade. Their spatial resolution being far beyond the diffraction limit [3] are able to probe the electromagnetic (EM) fields at the same length scale of the artificial patterning as well as to detect the untravelling waves in the far-field, namely, the evanescent and leaky waves. The recent works in this field have reported different detection schemes and nearfield probes morphologies allowing the observation of the electric [4] and magnetic [5] components of the EM fields and revealing their complex amplitudes [6] or their intensities as well as their temporal dynamics [7]. However, all these approaches suffer from a short spectral range, limited by the frequency shifters bandwidth in the interferomeric schemes and by the availability of commercial laser sources in any case. As discussed earlier, the versatile properties of the artificial materials over the spectrum would also require a broadband near-field detection scheme able to quantify the dispersion of the EM fields inside them. This issue is addressed here by developing a hyperspectral scanning nearfield optical microscope (Hyp-SNOM). Using a broadband illumination and detection as proposed at visible wavelengths in plasmonics [8], the Hyp-SNOM used here enables the direct observation of light dispersion within an on-chip integrated graded photonic crystal operating at near-infrared wavelengths. To provide an overview of the capabilities of the near-field technique reported here, the fascinating mirage effect [9] is directly visualized in the optical near-field of a two dimensional graded photonic crystal (GPhC). The spectral and spatial dispersions of curved light beams are then quantified experimentally and compared quantitatively to three dimensional plane wave assisted Hamiltonian optics2 (HO) predictions of light propagation.

Using the Hyp-SNOM, we directly measured the light propagation and dispersion inside the GPhC for a TE polarization. For silicon based materials, only near-infrared wavelengths above the Si electronic bandgap propagate inside the SOI chip, and the near-field detection is thus restricted to the 1200-1650nm spectral range. As a result, the hyperspectral matrix is recorded in 30 minutes with a 290nm spatial resolution over a 45x90µm image and with a 1nm spectral resolution over the total spectral range. Then different representations of the matrix permit to emphasize the spatial or the spectral properties of the GPhC.

A conventional approach to project the hyperspectral matrix is the representation of the EM field maps at selected wavelengths. As shown in Figures 2(b)–3(e), this provides for the first time the direct experimental proof of the mirage effect due to the gradual nature of the PhC. The mirage effect takes place at wavelengths from 1450 nm to1650 nm. In this range, the chromatic dispersion of this effect is clearly evidenced by the progressive penetration of the light

beam within the PhC area and the displacement of its curvature while increasing the wavelength. Another feature clearly visible here is the absence of spatial beam spreading over a main part of the spectrum, providing a direct proof of the light beam collimation all along the curved trajectories.

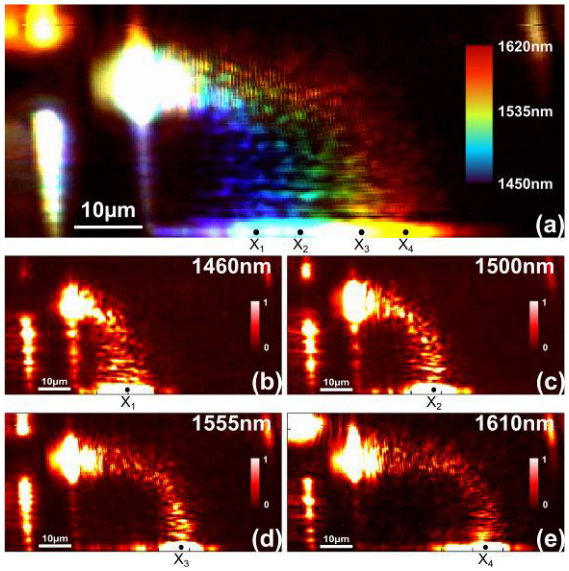

Fig. 1: SNOM images: a) hyperspectral image to provide an overall knowledge of the structure behaviour, b) c) d) e) field maps obtained in TE light polarization at λ=1460, 1500, 1555, 1610nm, respectively.

Then, mimicking the classical representation of light dispersion through a glass prism, the hyperspectral matrix can be plotted on a single "white" image by using a color coded scale over the spectral range where the mirage effect takes place (Figure 1(a)). As a result, this representation provides on a single image of the light rainbow due to the artificial material dispersion.

To quantitatively estimate the dispersion of the GPhC studied here, we directly resort to the analysis of the hyperspectral matrix. All along the GPhC area (namely, along the x-axis in the figures), we extracted the optical spectra. Four snapshots of the spectra at different x, corresponding to the x1 to x4 coordinates in Figure 1, are plotted in Figure 2(a). Each spectrum was then fitted by a Gaussian function to estimate its central wavelength as well as its spectral full width at half maximum (FWHM). Repeating this protocol all along the x-axis permits to extract the dispersion relationships plotted in Figures 2(b) and 2(c), which show the light beam position along the output interface in respect to the excitation wavelength. For each position, the spectral (Figure 2(b)) and spatial (Figure 2(c)) FWHMs of the light beam are superimposed by horizontal and vertical segments. As a result, it is found that the output beam shifts almost linearly with a slope of 0.25 µm/nm in the 1470–1600 nm spectral range without noticeable spatial or spectral spreading. This dispersion value is comparable to the one achievable, thanks to the PhC superprism effect [9] over almost the same propagation length about 0.4 µm/nm, but the strong beam spreading inherent to the superprism effect appears here drastically reduced.

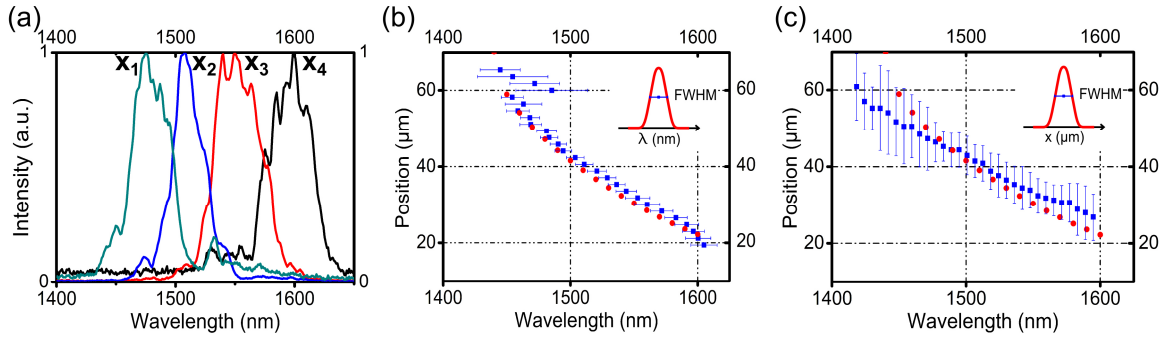

Fig. 2 : Quantitative estimation of the wavelength dispersion properties of the fabricated GPhC using Hyp-SNOM measurements: a) Spectral profiles recorded at the different coordinates depicted in figures. 3b)-to-e). Position of the centre of the output optical beam along the x-axis shown in figure 1 as a function of light wavelength: filled blue squares corresponds to Hyp-SNOM measurements b) with horizontal segments showing the beam FWHM spectral size, c) with vertical segments showing the beam FWHM spatial size; while red circles corresponds to Hamiltonian Optics calculations based on the GPhC bandstructure extraction after 3D-PWE calculations.

Thanks to the Hyp-SNOM results, we provide also a direct experimental observation of the transition between the diffraction and the homogenization regimes of light propagation. Figure 3 shows the Hyp-SNOM intensity image measured at λ=1420nm, which is characteristic of the observed phenomena. As seen in Figure 3, light propagation is

first characterized by a slightly upward bended path, whereas the last part of the light trajectory is directed downward. The beginning upward bending of the light path can be easily related to conventional mirage effect in the Long Wavelength Regime (LWR), in exact analogy with the atmospheric mirage effect where light trajectory is bended towards high index regions of graded index media. The monitored abrupt downward bending effect is thus the signature of a non-conventional mirage effect meaning that light propagation has then entered the Short Wavelength Regime. The transition between these two behaviours is interestingly fairly abrupt and occurs at a specific location (xth,yth) within the GPhC area that can be easily estimated from the SNOM image.

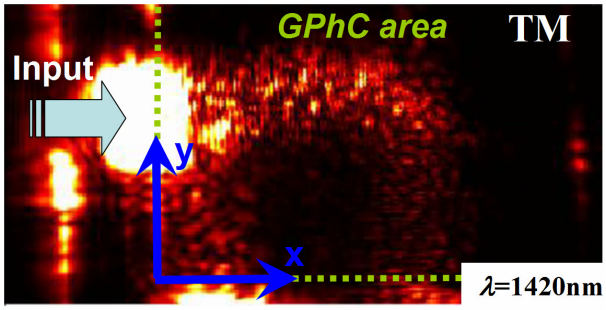

Fig. 3 : Optical near-field image of the light optical intensity propagation through the structure in TM polarization at λ=1420nm

The employed Hyp-SNOM experimental setup allowed us to exploit the images collected for other frequency values than 1420nm and repeat the estimation of (x_{th},y_{th}) in the full frequency range under investigation. Doing this, we extracted the local PhC filling factor for each (x_{th},y_{th}) threshold point, and then estimated the local long range index as a function of light wavelength. The related experimental ratio $\lambda/(n_{long\_range})_{\text{threshold}}$ is reported in Figure 4. From the near-field optical measurements, an invariant quantity is thus experimentally obtained that describes the transition between the LWR and the SWR. In the 1300nm-1490nm wavelength range, $\lambda/(n_{long\_range})_{\text{threshold}}$ is estimated to 677.4nm, i.e. only 1.78 times the lattice period a, with a standard deviation as low as 4.4nm.

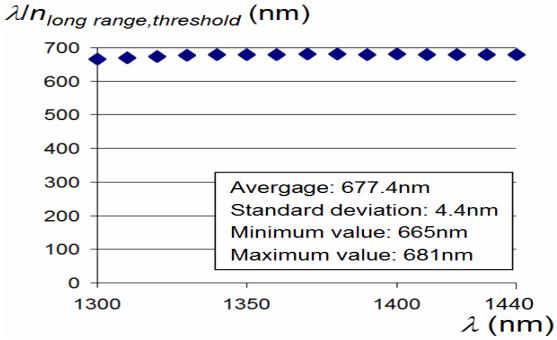

Fig 4 : Evolution of "λ/n" using a homogenized PhC index at the threshold position between the conventional the conventional and unconventional mirage effects.

In conclusion, we report here the experimental observation of the mirage effect in a graded photonic crystal and the transition between the LWR and SWR of light propagation.
The employed method allows a direct experimental investigation of the mirage effect and its dispersion over the 1200 nm–1650 nm spectral range, giving insight into the physics of dispersive electromagnetic phenomena in these unusual artificial optical materials.
Additionally, the reported abruptness of the LWR/SWR transition may also be of interest for the realization of original optical functionalities exploiting graded photonic crystals operating simultaneously in the two regimes of light propagation.

Références bibliographiques

[1] E. Cassan, K.V. Do, C. Caer, D. Marris-Morini, L. Vivien, Journal of Lightwave Technology 29 (13), 1937 (2011)
[2] K.-V. Do, X. Le Roux, D. Marris-Morini, L. Vivien, E. Cassan,, Optics Express 20 (14), 4476 (2012)
[3] D.W. Pohl, W. Denk, M. Lanz. App. Phys. Lett. 44, 651 (1984)
[4] L. Lalouat, B. Cluzel, C. Dumas, L. Salomon, F. de Fornel. Phys. Rev. B 83, 115326 (2011)
[5] M. Burresi, D. van Oosten, T. Kampfrath, H. Schoenmaker, R. Heideman, A. Leinse, L. Kuipers. Science 326, 550-553 (2009)
[6] M.L.M. Balistreri, J.P. Korterik, L. Kuipers, N.F. van Hulst. Phys. Rev. Lett. 85,294 (2000)
[7] R J. P.Engelen, Y. Sugimoto,H. Gersen, N. Ikeda, K. Asakawa, L. Kuipers. Nature Physics 3, 401 – 405 (2007)
[8] J.S. Bouillard, S. Vilain, W. Dickson, A.V. Zayats. Optics Express 18, 16513-16519 (2010)
[9] J. Dellinger, D. Bernier, B. Cluzel, X. le Roux, A. Lupu, F. de Fornel, E. Cassan. Opt. Lett. 36, 1074–1076 (2011)